Fast and Accurate Antenna Pattern Evaluation from Near-Field Data Acquired via Planar Spiral Scanning

Francesco D'Agostino, *Member, IEEE,* Flaminio Ferrara, *Member, IEEE,* Claudio Gennarelli, *Senior Member, IEEE,* Rocco Guerriero, *Member, IEEE,* Scott McBride, and Massimo Migliozzi

***Abstract*—Two fast and accurate probe compensated planar spiral near-field – far-field (NF–FF) transformation techniques, using nonredundant NF data, are experimentally assessed. These techniques allow a remarkable measurement time saving since they require a reduced number of NF data, which are collected on fly by properly and continuously moving the positioners. They have been achieved by applying the unified theory of spiral scannings for nonvolumetric antennas and adopting either an oblate ellipsoid or a double bowl to shape an antenna with a quasi-planar geometry. By using these modelings, instead of the spherical one, it is possible to significantly reduce the error due to the truncation of the scanning zone, since the NF data can be acquired on a spiral lying on a plane located at a distance smaller than one half of the antenna maximum size. The NF data required by the standard plane-rectangular NF–FF transformation are then accurately recovered from those collected along the spiral. Some experimental results, obtained at the UNISA Antenna Characterization Lab and assessing the effectiveness of the techniques, are shown.**

***Index Terms*—Antenna measurements, near-field – far-field transformation techniques, nonredundant sampling representations, optimal sampling interpolation, planar spiral scanning.**

I. Introduction

As is well known, the precise measurement of the antenna radiation characteristics can be performed only in an anechoic chamber, which ensures the free-space propagation conditions by practically eliminating the reflections from the floor, ceiling, and lateral walls. Unfortunately, when considering antennas with large dimensions in terms of wavelenghts, the Fraunhofer distance requirements are not fulfilled in an anechoic chamber. In such a case, a very convenient alternative to indoor compact range measurements or direct far-field (FF) measurements performed on an outdoor FF range is the utilization of near-field – far-field (NF–FF) transformations [1]-[3], allowing an accurate FF pattern reconstruction of the antenna under test (AUT) from the NF measurements. Among these transformations, those employing the classical plane-rectangular [4], [5] or plane-polar scannings [6], [7] are tailored for high gain antennas characterized by pencil beam patterns. From the mechanical viewpoint, this last scan is simpler than the plane-rectangular one, because it is achieved by means of a linear displacement of the probe and a rotational movement of the AUT. Moreover, it allows one to cover a scanning zone greater than in the plane-rectangular case, for a fixed size of the anechoic chamber. However, its former approach [6] required a large computational time to recover the antenna FF pattern. Such a shortcoming has been surmounted in [7] by applying the simple bivariate Lagrange interpolation for recovering the plane-rectangular NF data from the acquired plane-polar ones, thus taking full advantage of the fast Fourier transform (FFT) algorithm to evaluate the far field. However, due to the generic nature of this technique, very close spacings were required to make negligible the interpolation error. By exploiting the spatial quasi-bandlimitation properties of electromagnetic (EM) fields [8] and using the optimal sampling interpolation (OSI) expansions, a more efficient interpolation scheme, requiring a significantly lower number of data, has been developed in [9].

The measurement time saving is currently one of the most relevant issue related to the NF-FF transformation techniques, since the acquisition time is very much greater than the computational one needed to perform the transformation. To this end, the nonredundant sampling representations of EM fields [10], [11] have been properly exploited in [12], [13] and [14]-[16] to achieve a huge decrease in the NF data number in the plane-rectangular and plane-polar scanning, respectively. Another effective option to reduce the measurement time is, as suggested in [17], speeding up the NF data acquisition by means of continuous and synchronized movements of the involved positioners. In particular, planar spiral NF-FF transformations, which maintain all the advantages of the plane-polar ones, have been developed in [17]-[22]. Among these transformations, those [19]-[22] exploiting the nonredundant sampling representations are even more efficient from the measurement time reduction viewpoint, since they require a minimum number of NF data and spiral turns (Fig. 1). The data for carrying out the

Manuscript received February 24, 2016.

F. D'Agostino, F. Ferrara, C. Gennarelli, R. Guerriero, and M. Migliozzi are with the Department of Industrial Engineering, University of Salerno, 84084 Fisciano (SA), Italy (e-mail: fdagostino@unisa.it; flferrara@unisa.it; cgennarelli@unisa.it; rguerriero@unisa.it; mmigliozzi @unisa.it).

S. McBride is with MI Technologies, Suwanee, Georgia 30024, USA (e-mail: smcbride@mitechnologies.com).

NF-FF transformation with plane-rectangular scan [5] are then efficiently retrieved from the nonredundant spiral ones by employing proper OSI expansions. Recently, NF-FF transformations using NF data acquired along a helix or a spherical spiral have been developed too. The interested reader can find in [23] an exhaustive bibliography. The nonredundant representations for the probe response (voltage) over the plane and the related OSI expansions have been obtained by modeling the antenna with a sphere [19], [20], an oblate ellipsoid [21], or a double bowl (i.e., a surface consisting of two circular bowls having an identical aperture and possibly different lateral bends) [22]. According to the unified theory of spiral scans for nonspherical antennas [22], the scanning spiral has been determined in order to allow a two-dimensional interpolation. Therefore, its pitch must coincide with the spacing relevant to the radial line interpolation. Then, a voltage representation on the spiral, using a nonredundant number of samples, has been developed. It must be stressed that, when considering antennas having a quasi-planar geometry, the oblate ellipsoidal and double bowl AUT modelings are more effective than that adopting a sphere. As a matter of fact, they reduce the volumetric redundancy of the spherical modeling for these antennas and allow one to locate the scanning plane at a distance less than one half of the antenna maximum dimension, thus lowering the error due to the measurement surface truncation.

The aim of the paper is just to provide the experimental assessment of the NF-FF transformations with planar spiral scan for quasi-planar antennas based on the oblate ellipsoidal [21] and double bowl [22] modelings of the AUT (see Figs. 2 and 3, respectively). The experimental validation has been performed in the Antenna Characterization Lab of the University of Salerno, equipped with a plane-polar NF scanning system supplied by MI Technologies.

The paper is organized as follows. The nonredundant representation of the probe voltage over a plane from its samples collected on a spiral and the related OSI expansion are presented in Section II. The optimal parameters of such a representation are specified in the subsequent section for various AUT modelings. The key steps of the plane-rectangular NF-FF transformation when using an open-ended rectangular waveguide as probe are reported in Section IV. Exhaustive experimental results validating the effectiveness of the proposed techniques are shown in Section V. Conclusions are finally drawn in Section VI.

II. Nonredundant Voltage Representation on a Plane

Let an AUT be considered as enclosed in a rotational surface Σ bordering a convex domain and the voltage be measured by a nondirective probe moving along a planar spiral at $z = d$, with (x, y, z) being a Cartesian coordinate system with the origin at the AUT centre (Fig. 1). A spherical reference system (r, ϑ, φ) is employed for denoting any observation point, whereas a point P lying on the plane can be also identified by the plane-polar coordinates (ρ, φ). The voltage measured by such a probe has the same effective spatial bandwidth as the field radiated by the AUT [24] and, therefore, the theoretical results in [10] can

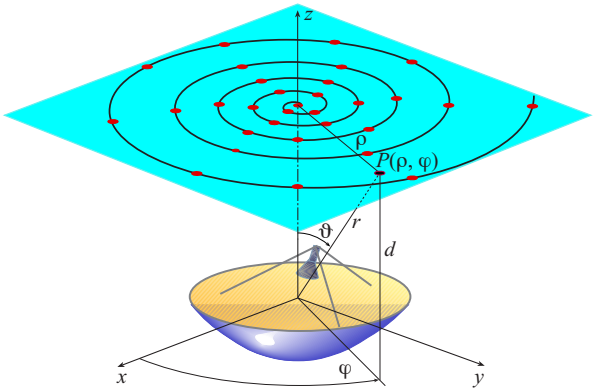

Fig. 1. Planar spiral scanning.

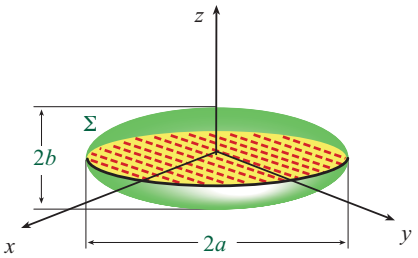

Fig. 2. Oblate ellipsoidal AUT modeling.

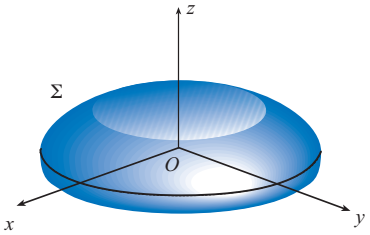

Fig. 3. Double bowl AUT modeling.

be properly exploited to get a nonredundant sampling representations for it. Accordingly, when dealing with its representation over a curve C lying on the plane, it is convenient to introduce the "reduced voltage"

$$\tilde{V}(\eta) = V(\eta) e^{j\psi(\eta)} \tag{1}$$

where η is the optimal parameter adopted for describing C, $\psi(\eta)$ is an appropriate phase function, and $V(\eta)$ is the voltage measured by the probe (V_φ) or by the rotated probe (V_ρ). Because $\tilde{V}(\eta)$ is not rigorously spatially bandlimited, an error occurs when approximating it with a bandlimited function. In any case, such an error approaches very small values as the bandwidth becomes greater than the threshold W_η [10]. Therefore, it can be effectively reduced by imposing that the approximating function has a properly increased bandwidth $\chi' W_\eta$, χ' being an excess bandwidth factor slightly greater than unity for electrically large antennas [8]. As shown in [10], the surface Σ must fit very well the AUT geometry in order to optimally reduce the required number of samples.

As suggested by the unified theory of spiral scans for nonvolumetric antennas [22], the voltage on the plane can be effi-

ciently reconstructed from a nonredundant number of its samples acquired on the spiral by means of a two-dimensional OSI expansion, achieved by determining the spiral whose step coincides with the spacing needed for interpolating on a radial line and deriving an appropriate nonredundant sampling representation over such a spiral.

The bandwidth, the optimal parameterization and phase function relevant to a radial line are [10], [22]:

$$W_\eta = \beta \ell' / 2\pi \tag{2}$$

$$\eta = (\pi/\ell')\left[R_1 - R_2 + s_1' + s_2'\right] \tag{3}$$

$$\psi = (\beta/2)\left[R_1 + R_2 + s_1' - s_2'\right] \tag{4}$$

where ℓ' is the length of the curve C' (intersection between Σ and the meridian plane through the observation point P), β the free-space wavenumber, $R_{1,2}$ the distances between P and the tangency points $P_{1,2}$ on C', and $s_{1,2}'$ the corresponding curvilinear abscissas.

The sample spacing required for interpolating on a radial line and, as a consequence, the pitch of the spiral is then $\Delta\eta = 2\pi/(2N''+1)$, where $N'' = \mathrm{Int}(\chi N') + 1$, $\mathrm{Int}(x)$ denotes the integer part of x, $N' = \mathrm{Int}(\chi' W_\eta) + 1$, and $\chi > 1$ is an oversampling factor, which controls the truncation error [10]. Thus, the spiral equations are:

$$\begin{cases} x = \rho(\eta)\cos\phi \\ y = \rho(\eta)\sin\phi \\ z = d \end{cases} \tag{5}$$

where $\rho(\eta) = d\tan\theta(\eta)$ and the parameters ϕ and η are related by:

$$\eta = k\phi \tag{6}$$

Accordingly, since the pitch is determined by two successive intersections of the spiral with a radial line, it results that $k = 1/(2N''+1)$ [22]. It is useful to note that θ, unlike the zenithal angle ϑ, can assume also negative values and that the azimuthal angle φ has a discontinuity jump of π when the spiral crosses the pole, while the spiral angle ϕ is always continuous. At last, it is noteworthy that the scanning spiral can be viewed as obtained by projecting on the plane, via the curves at η = constant, a spiral wrapping with the same pitch the surface Σ modeling the AUT.

The unified theory of spiral scannings for nonvolumetric antennas [22] shows also the way to derive the nonredundant representation along the spiral. The optimal parameter ξ for describing the spiral and the related phase function γ are determined as follows: ξ is equal to β/W_ξ times the arclength of the projecting point lying on the spiral that wraps the surface Σ, whereas γ coincides with the phase function ψ relevant to a radial line. As regards the bandwidth W_ξ, it is chosen in such a way that the parameter ξ spans a 2π range when the entire (closed) projecting spiral is drawn. Then, W_ξ is β/π times the length of the spiral that wraps Σ from pole to pole [22].

According to these results, the voltage at the point P on the radial line at φ can be reconstructed [21] by the OSI expansion:

$$V(\eta(\vartheta),\varphi) = \mathrm{e}^{-\mathrm{j}\psi(\eta)} \sum_{n=n_0-q+1}^{n_0+q} \tilde{V}(\eta_n) G(\eta,\eta_n,\overline{\eta},N,N'') \tag{7}$$

where $2q$ is the number of the retained intermediate samples $\tilde{V}(\eta_n)$, namely those at the intersections between the radial line through P and the spiral, $n_0 = \mathrm{Int}[(\eta-\eta_0)/\Delta\eta]$, and

$$\eta_n = \eta_n(\varphi) = k\varphi + n\Delta\eta = \eta_0 + n\Delta\eta \tag{8}$$

In (7),

$$G(\eta,\eta_n,\overline{\eta},N,N'') = D_{N''}(\eta-\eta_n)\,\Omega_N(\eta-\eta_n,\overline{\eta}) \tag{9}$$

where

$$D_{N''}(\eta) = \frac{\sin\left((2N''+1)\eta/2\right)}{(2N''+1)\sin(\eta/2)} \tag{10}$$

$$\Omega_N(\eta,\overline{\eta}) = \frac{T_N\left[2(\cos(\eta/2)/\cos(\overline{\eta}/2))^2 - 1\right]}{T_N\left[2/\cos^2(\overline{\eta}/2) - 1\right]} \tag{11}$$

are the Dirichlet and Tschebyscheff sampling functions [10], [21], with $T_N(\eta)$ being the Tschebyscheff polynomial of degree $N = N'' - N'$ and $\overline{\eta} = q\Delta\eta$.

The intermediate samples $\tilde{V}(\eta_n)$ are determined [21] via the following OSI expansion along the spiral:

$$\tilde{V}(\xi(\eta_n)) = \sum_{m=m_0-p+1}^{m_0+p} \tilde{V}(\xi_m) G(\xi(\eta_n),\xi_m,\overline{\xi},M,M'') \tag{12}$$

where $m_0 = \mathrm{Int}[\xi(\eta_n)/\Delta\xi]$, $2p$ is the retained samples number, $\overline{\xi} = p\Delta\xi$, $M = M'' - M'$, and

$$\xi_m = m\Delta\xi = 2\pi m/(2M''+1) \tag{13}$$

being $M'' = \mathrm{Int}[\chi M'] + 1$ and $M' = \mathrm{Int}[\chi' W_\xi] + 1$.

Since small changes of ξ give rise to large variations of ϕ in the zone close to the pole ($\vartheta = 0$), a properly increased excess bandwidth factor χ' must be considered to prevent that the band-limitation error grows significantly in such a zone [21].

A realistic example of a scanning spiral with the related sampling points arrangement is shown in Fig. 4. As can be seen, the spiral step increases moving away from the center, as well as the spacing between two consecutive samples. In the figure, the spiral turns beyond the pole, providing the required guard samples, are depicted in red and the related samples are shown with crosses instead of points. The denser samples distribution around the pole, due to the required increasing of χ' in this zone, is also visible.

The voltages V_φ or V_ρ at the points required by the classical probe corrected NF-FF transformation with plane-rectangular scan [5] can be then accurately determined by properly exploiting (7) and (12). Unfortunately, the probe must maintain its orientation with respect to the AUT in order that the formulas in [5] be valid, so that it must co-rotate with the AUT. A probe

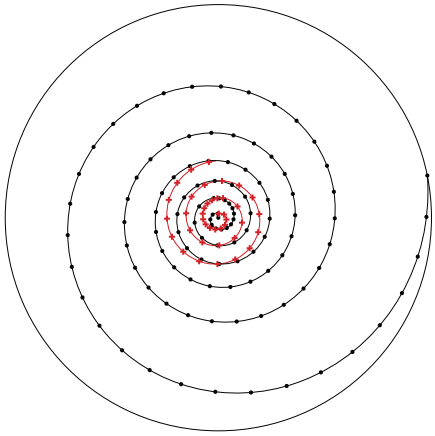

Fig. 4. Spiral sampling arrangement.

characterized by a far field with a first-order φ-dependence can be properly employed to avoid the co-rotation. In fact, in this case, the measured voltages V_φ and V_ρ are related to the corresponding co-rotated ones V_P and V_R by:

$$V_P = V_\varphi \cos\varphi - V_\rho \sin\varphi\,; \qquad V_R = V_\varphi \sin\varphi + V_\rho \cos\varphi \tag{14}$$

In Section IV, the probe corrected formulas relevant to the NF-FF transformation with plane-rectangular scan and the probe characterization of an open-ended rectangular waveguide, which exhibits the above characteristics when excited by a TE_{10} mode, are reported for reader's convenience.

III. Antenna Modelings

Any arbitrary finite size radiating source can always be considered as enclosed in the smallest sphere of radius a able to contain it (spherical antenna modeling). In such a case, as shown in [19]-[22], it results:

$$W_\eta = \beta a\,; \qquad \eta = \theta \tag{15}$$

$$\psi = \beta\sqrt{r^2 - a^2} - \beta a \cos^{-1}(a/r) \tag{16}$$

and the projecting curves at η = constant are radial lines.

The spherical modeling is the easiest to use and understand of the three AUT models described herein. However, its use is no longer convenient when considering antennas having a quasi-planar geometry, which usually are those characterized in a planar NF facility. In fact, it prevents to locate the measurement plane at a distance less than one half of the antenna maximum size, and this gives rise to an increase of the error due to the truncation of the scanning surface. Moreover, the redundancy of the spherical modeling implies an ineffective increase of the required NF samples number.

For a quasi-planar AUT, a convenient modeling is achieved by choosing the smallest oblate ellipsoid, having semi-major and semi-minor axes equal to a and b (Fig. 2), as surface Σ containing it. A huge decrease in the number of the required NF data, as well as a reduction of the distance of the measurement plane, can be so achieved. In fact, the plane must be, now, outside an oblate ellipsoid with semi-minor axis b, instead of a sphere with radius a. In such a case, as shown in [10], [21], it results:

$$W_\eta = (4a/\lambda)\, E\left(\pi/2 \middle| \varepsilon^2\right) \tag{17}$$

$$\eta = (\pi/2)\left[E\left(\sin^{-1}u \middle| \varepsilon^2\right) \Big/ E\left(\pi/2 \middle| \varepsilon^2\right)\right] \tag{18}$$

$$\psi = \beta a\left[v\sqrt{\frac{v^2-1}{v^2-\varepsilon^2}} - E\left(\cos^{-1}\sqrt{\frac{1-\varepsilon^2}{v^2-\varepsilon^2}}\,\middle|\, \varepsilon^2\right)\right] \tag{19}$$

wherein λ is the wavelength, $E(\bullet\,|\,\bullet)$ denotes the elliptic integral of second kind, $u = (r_1 - r_2)/2f$ and $v = (r_1 + r_2)/2a$ are the elliptic coordinates, $r_{1,2}$ being the distances from the observation point P to the foci of the ellipse C', and f the semi-interfocal distance. Moreover, $\varepsilon = f/a$ is the eccentricity of C'. It is noteworthy that the projecting curves at η = constant are no longer the radial lines of the spherical modeling, but hyperbolas confocal to the ellipse C'. It must be stressed that the oblate ellipsoidal model contains the spherical one as particular case. In fact, when $b = a$, the ellipsoid becomes a sphere and relations (15), (16) are easily obtained from the general ones (17)-(19).

Another modeling for quasi-planar antennas is got by choosing as surface Σ a double bowl, consisting of two circular bowls with identical aperture diameter $2a$. The radii c and c' of its upper and lower arcs may differ for a better fitting of the AUT shape (Figs. 3 and 5). In this case, the expressions of W_η, η, and ψ are obtained from (2)-(4) by taking into account that $\ell' = 2\left[(a-c)+(a-c')+(c+c')\pi/2\right]$ and substituting in them the proper values of the distances $R_{1,2}$ and curvilinear abscissas $s'_{1,2}$, which change depending on the position of the tangency points $P_{1,2}$ (Fig. 5). Note that, if $\rho < a$, these points are located on the upper bowl, whereas P_2 is on the lower one, when $\rho > a$. Therefore, for $\rho \le a$, we get [22]:

$$R_1 = \sqrt{(\rho+b)^2 + d^2 - c^2}\,; \qquad s'_1 = -(b + c\alpha_1) \tag{20}$$

$$\alpha_1 = \tan^{-1}(R_1/c) - \tan^{-1}\left[(\rho+b)/d\right]; \qquad b = a - c \tag{21}$$

$$R_2 = \sqrt{(b-\rho)^2 + d^2 - c^2}\,; \qquad s'_2 = b + c\alpha_2 \tag{22}$$

$$\alpha_2 = \tan^{-1}(R_2/c) - \tan^{-1}\left[(b-\rho)/d\right] \tag{23}$$

and, for $\rho > a$, R_1, s'_1, and α_1 can be again evaluated by means of relations (20) and (21), whereas it results [22]:

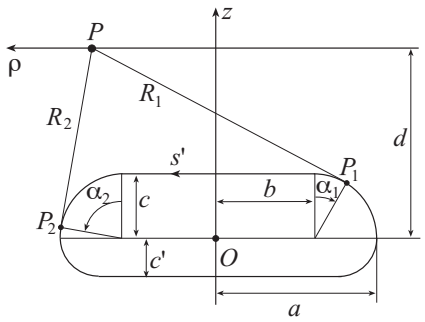

Fig. 5. Geometry of the double bowl AUT modeling.

$$R_2 = \sqrt{(\rho - b')^2 + d^2 - c'^2}\ ; \qquad s_2' = b + c\pi/2 + c'\alpha_2 \quad (24)$$

$$\alpha_2 = \tan^{-1}(R_2/c') - \pi/2 + \tan^{-1}[(\rho - b')/d]\ ; \quad b' = a - c' \quad (25)$$

It must be stressed that the spherical modeling can be obtained from the double bowl one by setting $c = c' = a$.

A brief discussion about which of the two described AUT modelings for quasi-planar antennas can be conveniently chosen now follows. Since the overall number of NF samples on any closed observation surface (also unbounded) surrounding the antenna is equal to the area of the surface Σ enclosing it [10], the proper modeling to reduce as much as possible the number of required samples is that minimizing such an area. In any case, the representation adopting the ellipsoidal oblate modeling is simpler than that using the two-bowl one, since the related expressions are in closed form. On the other hand, the latter is more flexible, since it allows one to better fit antennas characterized by a non-symmetrical extension with respect to the plane identified by their maximum transverse dimension.

IV. Plane-Rectangular NF-FF Transformation

The probe-corrected version [5] of the plane-rectangular NF-FF transformation relies on the Lorentz reciprocity theorem. For reader's convenience, the basic formulas in the considered reference system are reported in the following:

$$E_\vartheta(\vartheta,\varphi) = \left(I_R E'_{\varphi_P}(\vartheta,-\varphi) - I_P E'_{\varphi_R}(\vartheta,-\varphi)\right)\Big/\Delta \quad (26)$$

$$E_\varphi(\vartheta,\varphi) = \left(I_R E'_{\vartheta_P}(\vartheta,-\varphi) - I_P E'_{\vartheta_R}(\vartheta,-\varphi)\right)\Big/\Delta \quad (27)$$

where

$$\Delta = E'_{\vartheta_R}(\vartheta,-\varphi)E'_{\varphi_P}(\vartheta,-\varphi) - E'_{\vartheta_P}(\vartheta,-\varphi)E'_{\varphi_R}(\vartheta,-\varphi) \quad (28)$$

$$I_{P,R} = A\cos\vartheta\, e^{j\beta d\cos\vartheta} \cdot \int_{-\infty}^{+\infty}\int_{-\infty}^{+\infty} V_{P,R}(x,y)\, e^{j\beta x\sin\vartheta\cos\varphi}\, e^{j\beta y\sin\vartheta\sin\varphi}\, dx\, dy \quad (29)$$

A being a proper constant.

In relations (26) - (28), E'_{ϑ_P} and E'_{φ_P} are the FF components radiated by the probe, whereas E'_{ϑ_R} and E'_{φ_R} are those radiated by the rotated probe, when they are employed as transmitting antennas.

According to [25], the FF components of the electric field, $E'_{\vartheta P}$, E'_{φ_P}, radiated by an open-ended rectangular waveguide (of sizes a' and b' along x and y) excited by a TE_{10} mode are:

$$E'_{\vartheta_P} = f_\vartheta(\vartheta)\sin\varphi\frac{e^{-j\beta r}}{r} = A_E\frac{1+(k_z/\beta)\cos\vartheta}{1+(k_z/\beta)}\frac{\sin[\beta(b'/2)\sin\vartheta]}{\beta(b'/2)\sin\vartheta}\sin\varphi\frac{e^{-j\beta r}}{r} \quad (30)$$

$$E'_{\varphi_P} = f_\varphi(\vartheta)\cos\varphi\frac{e^{-j\beta r}}{r} = A_H\cos[\beta(a'/2)\sin\vartheta]\cdot \left\{\frac{\cos\vartheta + (k_z/\beta) + \Gamma[\cos\vartheta - (k_z/\beta)]}{(\pi/2)^2 - [\beta(a'/2)\sin\vartheta]^2} + C_0\right\}\cos\varphi\frac{e^{-j\beta r}}{r} \quad (31)$$

where

$$A_E = A_H\left\{\frac{4}{\pi^2}[1 + (k_z/\beta) + \Gamma(1 - (k_z/\beta))] + C_0\right\} \quad (32)$$

$$A_H = -j\beta^2 a' b' E_0/8 \quad (33)$$

$k_z = [\beta^2 - (\pi/a')^2]^{1/2}$ is the propagation constant of the TE_{10} mode, E_0 is its amplitude, and Γ is the reflection coefficient at the end of the waveguide, whose measured values are reported in [25]. Moreover, C_0 is a real constant which can be numerically evaluated [25].

It can be easily verified that:

$$E'_{\vartheta_R} = f_\vartheta(\vartheta)\cos\varphi\frac{e^{-j\beta r}}{r} \quad (34)$$

$$E'_{\varphi_R} = -f_\varphi(\vartheta)\sin\varphi\frac{e^{-j\beta r}}{r} \quad (35)$$

V. Experimental Validation

The experimental validation of the described planar spiral NF-FF transformations is provided in this section. The tests have been carried out in the anechoic chamber of the UNISA Antenna Characterization Lab, which is provided with a plane-polar NF facility system, besides the cylindrical and spherical ones, all supplied by MI Technologies. The pyramidal absorbers covering the anechoic chamber walls ensure a reflectivity lower than – 40 dB. The planar spiral scanning is carried out by using the plane-polar NF facility, which has been realized by mounting the probe on a linear vertical positioner and the AUT on a rotator. The rotator is attached to an L–shaped bracket, mounted on a horizontal slide, so that the scanning plane distance can be properly changed. A vector network analyzer is employed in the set-up to perform the amplitude and phase measurements of the transmission coefficient S_{21}, which is related to the output voltage of the open-ended WR90 rectangular waveguide used as probe.

The first set of results (from Fig. 7 to Fig. 12) refers to the NF-FF transformation technique relying on the oblate ellipsoidal AUT modeling and to a planar slotted array by Rantec Microwave Systems Inc., operating at 9.3 GHz (AUT1), shown in Fig. 6. This array has a radius of about 23 cm and is placed on the plane z = 0. An oblate ellipsoid having semi-axes a = 23.5 cm and b = 8.1 cm has been chosen to fit it and the probe has acquired the voltages V_φ and V_ρ along a spiral lying on a plane at z = 18.3 cm and spanning a circle of radius 110 cm.

In order to validate the accuracy of the OSI formulas, the amplitudes of the interpolated voltages V_φ and V_ρ on the radial lines at φ = 90° and φ = 30° are reported in Figs. 7 and 8 together with those directly measured (references). The reconstructions of the phases of the corresponding more significant voltage are also shown in Figs. 9 and 10. As can be seen, the recon-

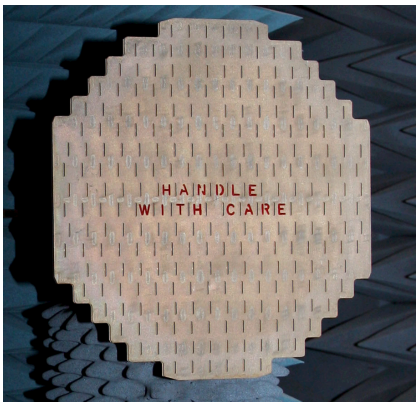

Fig. 6. Photo of the planar slotted array (AUT1).

structions are very good, save for the zone characterized by very low voltage levels (below about –60 dB), wherein the error is mainly due to the noise and the residual reflections from the anechoic chamber walls. It is noteworthy that the interpolated voltages exhibit a behaviour smoother than the directly measured ones, since the interpolating functions are able to reject the spatial harmonics of the noise exceeding the AUT spatial bandwidth, due to their low pass filtering properties. The above reconstructions have been got by choosing $\chi = 1.25$ and $p = q = 7$, which guarantee a truncation error smaller than the measurement one [21]. Moreover, to make the aliasing error negligible, an enlargement bandwidth factor equal to 1.25 has been employed, save for the zone of the spiral corresponding to the 24 samples centred on the pole, wherein such a factor has been further increased in such a way that the sample spacing is reduced by a factor 9.

The overall effectiveness of such a NF-FF transformation is assessed by comparing the FF patterns in the E- and H-planes (Figs. 11 and 12) reconstructed from the NF data collected along the spiral with those obtained by employing the NF cylindrical scanning facility. As can be seen, a good agreement results.

It must be stressed that the number of the acquired NF data is 2 197 (2 005 regular + 192 extra samples), about the same as that (1 987) needed by the plane-polar NF-FF transformation [15]. It must be pointed out that the number of plane-polar NF data needed by the approaches in [6], [7] is 29 105, whereas that required by the standard NF-FF transformation with plane-rectangular scanning [4], [5] is 18 769.

The interested reader can find in [26] other experimental results relevant to a different testing antenna, which further validate the efficiency of the NF-FF transformation based on the oblate ellipsoidal AUT modeling.

The second set of results (from Fig. 14 to Fig. 18) refers to a dual pyramidal horn antenna (AUT2) with horizontal polarization operating at 10 GHz and located on the plane $z = 0$. Each horn has a 6.8 cm × 8.9 cm sized aperture and the centre-to-centre distance between the apertures is 26 cm. A photo showing such an antenna, its mounting, the probe, and the rotator attached to the L–shaped bracket is reported in Fig. 13. Note that the photo has been taken before covering the rotator and AUT support with the necessary absorbers. The NF data have been acquired along a spiral lying on a plane at $z = 17$ cm and spanning a circle of radius 110 cm. A double bowl having $a = 18.6$ cm and $c = c' = 2.7$ cm has been adopted as AUT modeling. The amplitude and phase of the reconstructed voltage V_ρ

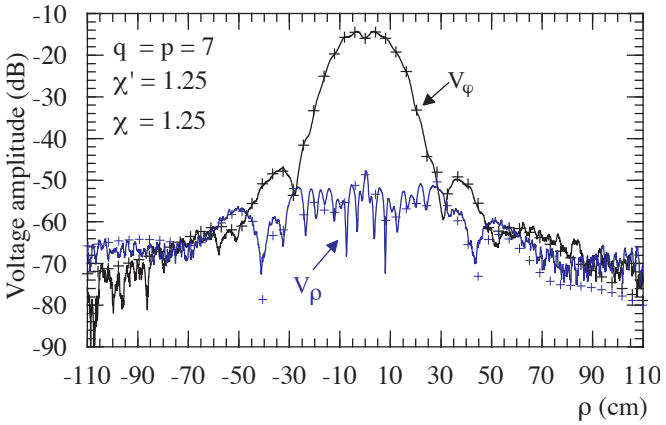

Fig. 7. Amplitudes of V_φ, V_ρ on the radial line at $\varphi = 90°$. Solid lines: references. Crosses: reconstructed from the planar spiral NF samples when the AUT1 is modeled by an oblate ellipsoid.

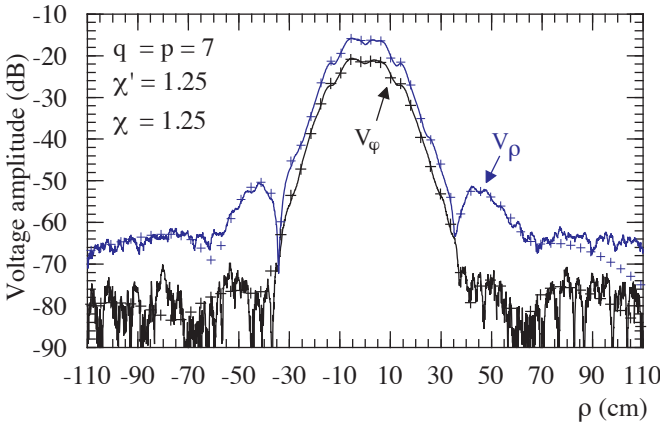

Fig. 8. Amplitudes of V_φ, V_ρ on the radial line at $\varphi = 30°$. Solid lines: references. Crosses: reconstructed from the planar spiral NF samples when the AUT1 is modeled by an oblate ellipsoid.

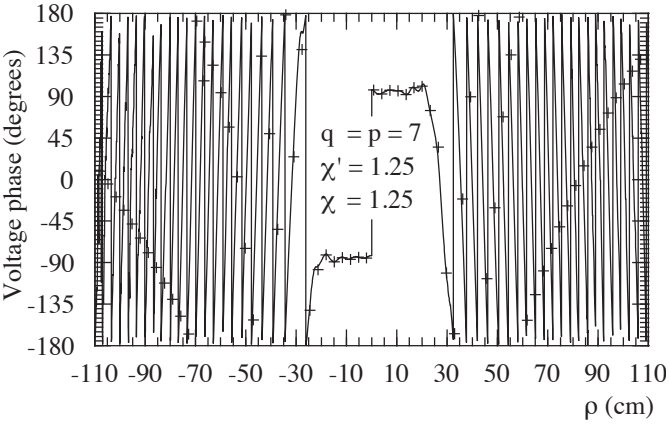

Fig. 9. Phase of V_φ on the radial line at $\varphi = 90°$. Solid line: reference. Crosses: reconstructed from the planar spiral NF samples when the AUT1 is modeled by an oblate ellipsoid.

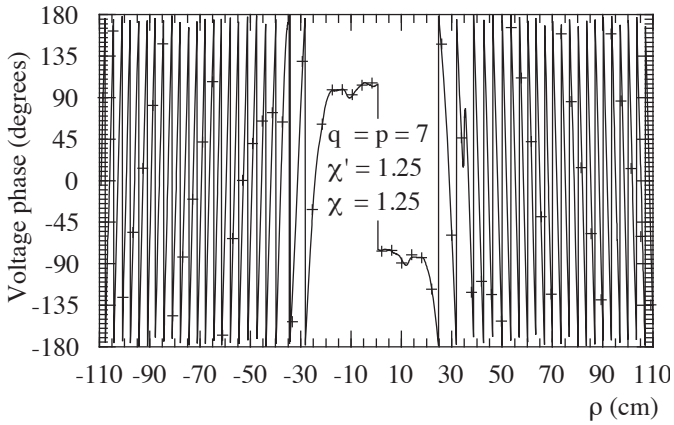

Fig. 10. Phase of V_ρ on the radial line at φ = 30°. Solid line: reference. Crosses: reconstructed from the planar spiral NF samples when the AUT1 is modeled by an oblate ellipsoid.

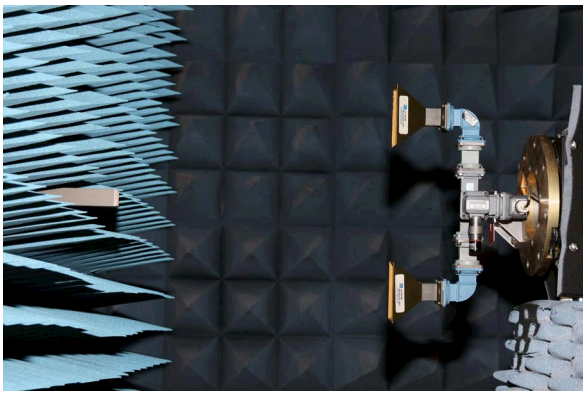

Fig. 13. Photo of the dual pyramidal horn antenna (AUT2) and of the UNISA planar NF facility.

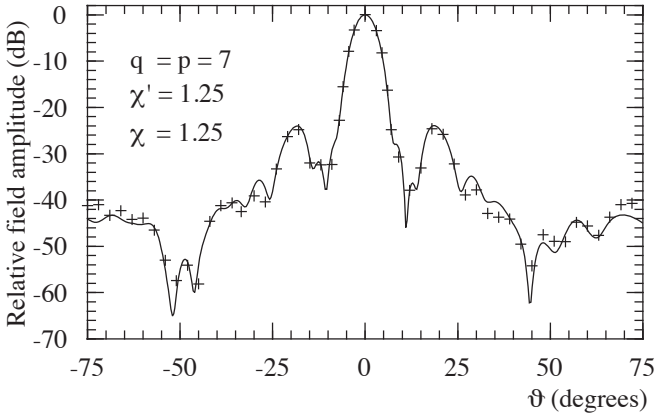

Fig. 11. FF pattern of AUT1 in the E-plane. Solid line: obtained from cylindrical NF data. Crosses: reconstructed via the planar spiral NF-FF transformation using the ellipsoidal AUT modeling.

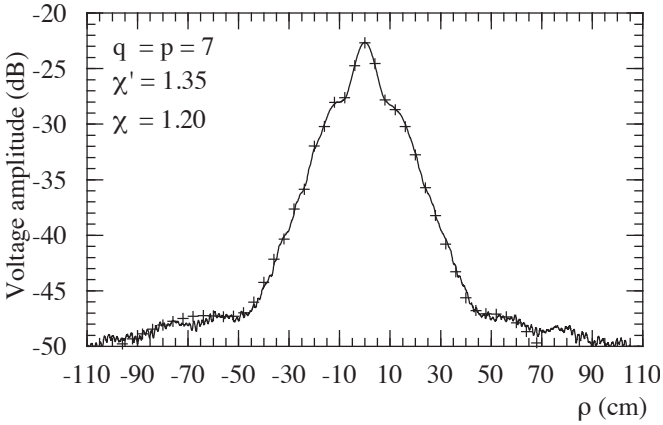

Fig. 14. Amplitude of V_ρ on the radial line at φ = 90°. Solid line: reference. Crosses: reconstructed from the planar spiral NF samples when the AUT2 is modeled by a double bowl.

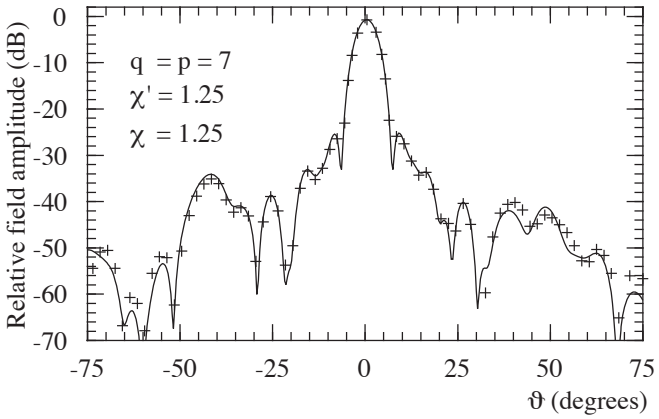

Fig. 12. FF pattern of AUT1 in the H-plane. Solid line: obtained from cylindrical NF data. Crosses: reconstructed via the planar spiral NF-FF transformation using the ellipsoidal AUT modeling.

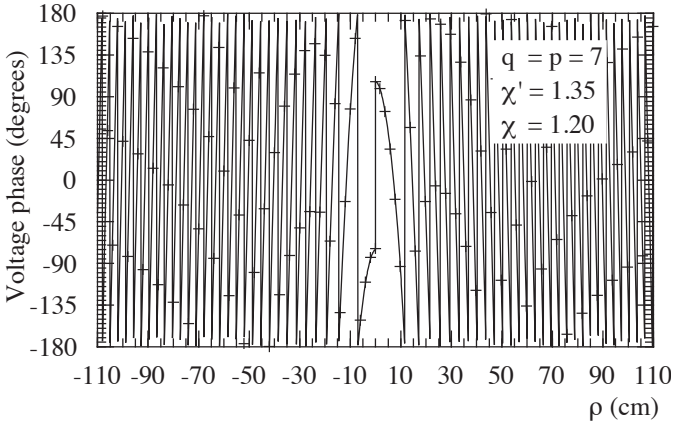

Fig. 15. Phase of V_ρ on the radial line at φ = 90°. Solid line: reference. Crosses: reconstructed from the planar spiral NF samples when the AUT2 is modeled by a double bowl.

on the radial line at φ = 90° are shown in Figs. 14 and 15 together with those directly measured (references). The comparison between the recovered and directly measured amplitudes of V_φ and V_ρ relevant to the radial line at φ = 30° is also reported in Fig. 16. These reconstructions have been obtained by using the same values of the OSI parameters χ, p, and q as in the previous set. In such a case, since the AUT is smaller, a χ' value equal to 1.35 has been adopted save for the zone of the spiral corresponding to the 24 samples around the pole, wherein it has been further increased in such a way that the sample spacing is

reduced by a factor 9. At last, the E- and H- plane patterns reconstructed from the NF spiral samples are compared (see Figs. 17 and 18) with the ones attained through the NF cylindrical scanning system. As can be seen, also when using the double bowl AUT modeling, very good NF and FF reconstructions have been obtained.

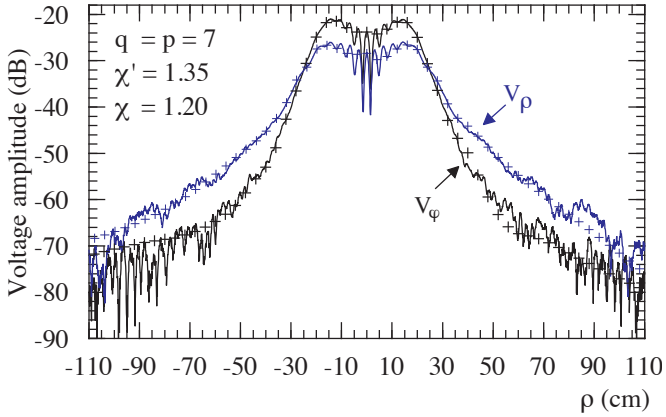

Fig. 16. Amplitudes of V_φ, V_ρ on the radial line at $\varphi = 30°$. Solid lines: references. Crosses: reconstructed from the planar spiral NF samples when the AUT2 is modeled by a double bowl.

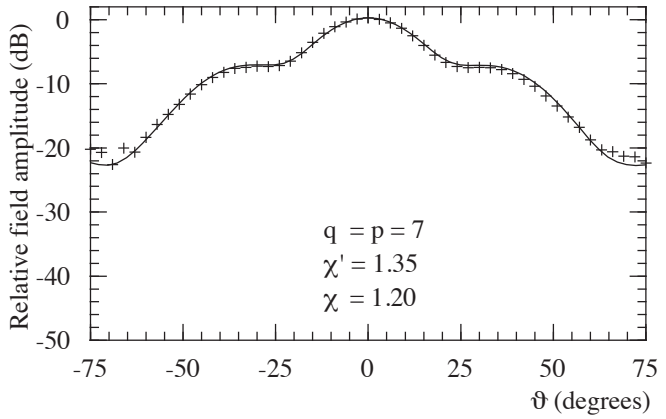

Fig. 17. FF pattern of AUT2 in the E-plane. Solid line: obtained from cylindrical NF data. Crosses: reconstructed via the planar spiral NF-FF transformation using the double bowl AUT modeling.

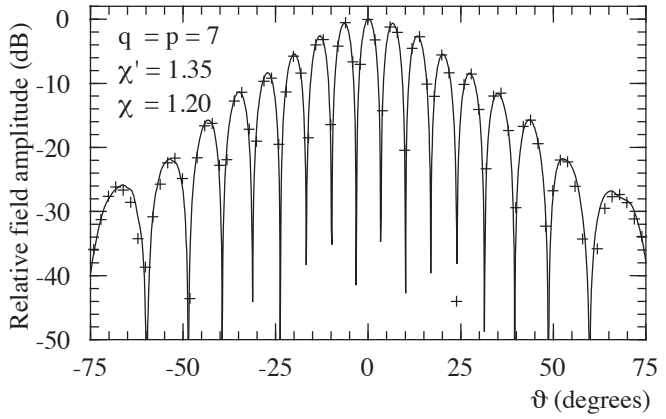

Fig. 18. FF pattern of AUT2 in the H-plane. Solid line: obtained from cylindrical NF data. Crosses: reconstructed via the planar spiral NF-FF transformation using the double bowl AUT modeling.

It is worth noting that the number of the used spiral samples is now 1 807 (1 615 regular + 192 extra samples), about the same as that (1 661) required by the nonredundant NF-FF transformation with plane-polar scan [14]. It must be pointed out that such a number is much smaller than the ones 33 581 and 21 609, needed by Rahmat-Samii's plane-polar NF-FF transformation [6], [7] and by the classical plane-rectangular one [4], [5], respectively.

VI. Conclusion

The experimental validation of the planar spiral NF-FF transformation techniques adopting either an oblate ellipsoid or a double bowl to model a quasi-planar antenna has been provided in this paper. The very good agreement found in the NF reconstructions, as well as that resulting from the comparison between the reconstructed FF patterns and those obtained by employing the cylindrical NF facility available at the UNISA Antenna Characterization Lab, has fully confirmed the effectiveness of the described NF-FF transformations also from the experimental point of view. For both the AUT models, the number of used NF data has resulted to be remarkably smaller than those needed by the standard plane-rectangular and plane-polar scans, thus showing that the NF-FF transformations employing such an innovative scanning allow a significant measurement time saving without any loss in accuracy.

References

[1] A. D. Yaghjian, "An overview of near-field antenna measurements," *IEEE Trans. Antennas Propag.*, vol. AP-34, no. 1, pp. 30-45, Jan. 1986.

[2] M. H. Francis and R. W. Wittmann, "Near-field scanning measurements: theory and practice," in *Modern Antenna Handbook*, C. A. Balanis, Ed., Hoboken, NJ, USA: John Wiley & Sons, Inc., 2008, pp. 929-976.

[3] M. H. Francis Ed., *IEEE Recommended Practice for Near-Field Antenna Measurements*, IEEE Standard 1720-2012.

[4] D. T. Paris, W. M. Leach, Jr., and E. B. Joy, "Basic theory of probe-compensated near-field measurements," *IEEE Trans. Antennas Propag.*, vol. AP-26, no. 3, pp. 373-379, May 1978.

[5] E. B. Joy, W. M. Leach, G. P. Rodrigue, and D.T. Paris, "Applications of probe-compensated near-field measurements," *IEEE Trans. Antennas Propag.*, vol. AP-26, no. 3, pp. 379-389, May 1978.

[6] Y. Rahmat-Samii, V. Galindo-Israel, and R. Mittra, "A plane-polar approach for far-field construction from near-field measurements," *IEEE Trans. Antennas Propag.*, vol. AP-28, no. 2, pp. 216-230, March 1980.

[7] M. S. Gatti and Y. Rahmat-Samii, "FFT applications to plane-polar near-field antenna measurements," *IEEE Trans. Antennas Propag.*, vol. 36, no. 6, pp. 781-791, June 1988.

[8] O. M. Bucci and G. Franceschetti, "On the spatial bandwidth of scattered fields," *IEEE Trans. Antennas Propag.*, vol. AP-35, no. 12, pp. 1445-1455, Dec. 1987.

[9] O. M. Bucci, C. Gennarelli, and C. Savarese, "Fast and accurate near-field–far-field transformation by sampling interpolation of plane-polar measurements," *IEEE Trans. Antennas Propag.*, vol. 39, no. 1, pp. 48-55, Jan. 1991.

[10] O. M. Bucci, C. Gennarelli, and C. Savarese, "Representation of electromagnetic fields over arbitrary surfaces by a finite and nonredundant number of samples," *IEEE Trans. Antennas Propag.*, vol. 46, no. 3, pp. 351-359, Mar. 1998.

[11] O.M. Bucci and C. Gennarelli, "Application of nonredundant sampling representations of electromagnetic fields to NF-FF transformation techniques," *Int. J. Antennas Propag.*, vol. 2012, ID 319856, 14 pages, 2012 [Online]. Available: http://www.hindawi.com/journals/ijap/2012/319856/

[12] F. Ferrara, C. Gennarelli, R. Guerriero, G. Riccio, and C. Savarese, "An efficient near-field to far-field transformation using the planar wide-mesh scanning," *J. Electromagn. Waves Appl.*, vol. 21, pp. 341-357, 2007.

[13] F. D'Agostino, I. De Colibus, F. Ferrara, C. Gennarelli, R. Guerriero, and M. Migliozzi, "Far-field pattern reconstruction from near-field data collected via a nonconventional plane-rectangular scanning: experimental testing," *Int. J. Antennas Propag.*, vol. 2014, ID 763687, 9 pages, 2014 [Online]. Available: http://www.hindawi.com/journals/ijap/2014/763687/

[14] O. M. Bucci, C. Gennarelli, G. Riccio, and C. Savarese, "Near-field–far-field transformation from nonredundant plane-polar data: effective modellings of the source," *IEE Proc. Microw. Antennas Propag.*, vol. 145, no. 1, pp. 33-38, Feb. 1998.

[15] O. M. Bucci, F. D'Agostino, C. Gennarelli, G. Riccio, and C. Savarese, "NF–FF transformation with plane-polar scanning: ellipsoidal modelling of the antenna," *Automatika*, vol. 41, no. 3-4, pp. 159-164, 2000.

[16] F. D'Agostino, F. Ferrara, C. Gennarelli, R. Guerriero, and M. Migliozzi, "An efficient NF-FF transformation technique with plane-polar scanning: experimental assessments," in *Proc. LAPC,* Loughborough, UK, 2014, pp. 231-235.

[17] R. G. Yaccarino, L. I. Williams, Y. Rahmat-Samii, "Linear spiral sampling for the bipolar planar antenna measurement technique," *IEEE Trans. Antennas Propag.*, vol. 44, no. 7, pp. 1049-1051, July 1996.

[18] S. Costanzo and G. Di Massa, "Near-field to far-field transformation with planar spiral scanning," *Prog. in Electromagn. Res.*, vol. 73, pp. 49-59, 2007 [Online]. Available: http://www.jpier.org/PIER/pier.php?paper=07031903

[19] O. M. Bucci, F. D'Agostino, C. Gennarelli, G. Riccio, and C. Savarese, "Probe compensated far-field reconstruction by near-field planar spiral scanning," *IEE Proc. Microw. Antennas Propag.*, vol. 149, no. 2, pp. 119–123, April 2002.

[20] F. D'Agostino, C. Gennarelli, G. Riccio, and C. Savarese, "Theoretical foundations of near-field–far-field transformations with spiral scannings," *Prog. in Electromagn. Res.*, vol. 61, pp. 193-214, 2006 [Online]. Available: http://www.jpier.org/PIER/pier.php?paper=0602141

[21] F. D'Agostino, F. Ferrara, C. Gennarelli, R. Guerriero, and M. Migliozzi, "An effective NF-FF transformation technique with planar spiral scanning tailored for quasi-planar antennas," *IEEE Trans. Antennas Propag.*, vol. 56, no. 9, pp. 2981-2987, Sept. 2008.

[22] F. D'Agostino, F. Ferrara, C. Gennarelli, R. Guerriero, and M. Migliozzi, "The unified theory of near–field–far–field transformations with spiral scannings for nonspherical antennas," *Prog. in Electromagn. Res. B*, vol. 14, pp. 449-477, 2009 [Online]. Available: http://www.jpier.org/PIERB/pier.php?paper=09031808

[23] R. Cicchetti, F. D'Agostino, F. Ferrara, C. Gennarelli, R. Guerriero, and M. Migliozzi, "Near-field to far-field transformation techniques with spiral scannings: a comprehensive review," *Int. J. Antennas Propag.*, vol. 2014, ID 143084, 2014 [Online]. Available: http://www.hindawi.com/journals/ijap/2014/143084/

[24] O .M. Bucci, G. D'Elia, and M. D. Migliore, "Advanced field interpolation from plane-polar samples: experimental verification," *IEEE Trans. Antennas Propag.*, vol. 46, no. 2, pp. 204-210, Feb. 1998.

[25] A. D. Yaghjian, "Approximate formulas for the far field and gain of open-ended rectangular waveguide," *IEEE Trans. Antennas Propag.*, vol. AP-32, no. 4, pp. 378-384, April 1984.

[26] F. D'Agostino, F. Ferrara, C. Gennarelli, R. Guerriero, and M. Migliozzi, "Pattern reconstruction from planar spiral near-field measurements @ UNISA Antenna Characterization Lab," in *Proc. ICEAA,* Turin, Italy, 2015, pp. 179-182.

Francesco D'Agostino (M'03) was born near Salerno (Italy) in 1965. He received the Laurea degree in electronic engineering from the University of Salerno in 1994, where in 2001 he received the Ph.D. degree in Information Engineering.

From 2002 to 2005, he was Assistant Professor at the Engineering Faculty of the University of Salerno where, in October 2005, he was appointed Associate Professor of Electromagnetics and joined the Department of Industrial Engineering, where he is currently working. His research activity includes application of sampling techniques to electromagnetics and to innovative NF–FF transformations, diffraction problems radar cross section evaluations, Electromagnetic Compatibility. In this area, Dr. D'Agostino has co-authored 4 books and over 150 scientific papers, published in peer-reviewed international journals and conference proceedings. He is a regular reviewer for several journals and conferences and has chaired some international events and conferences. Dr. D'Agostino is a member of AMTA and EurAAP.

Flaminio Ferrara (M'08) was born near Salerno, Italy, in 1972. He received the Laurea degree in electronic engineering from the University of Salerno in 1999.

Since the same year, he has been with the Research Group in Applied Electromagnetics at the University of Salerno. He received the Ph.D. degree in Information Engineering at the same University, where he is presently an Assistant Professor of Electromagnetic Fields. His interests include: application of sampling techniques to the efficient reconstruction of electromagnetic fields and to NF–FF transformation techniques; monostatic radar cross section evaluations of corner reflectors. Dr. Ferrara is co-author of more than 180 scientific papers, mainly in international journals and conference proceedings. He is reviewer for several international journals and member of the Editorial board of the *International Journal of Antennas and Propagation*.

Claudio Gennarelli (M'01-SM'02) was born in Avellino, Italy, in 1953. He received the Laurea degree (*summa cum laude*) in electronic engineering from the University of Naples, Italy, in 1978.

From 1978 to 1983, he worked with the Research Group in Electromagnetics at the Electronic Engineering Department of the University "Federico II" of Naples. In 1983, he became Assistant Professor at the Istituto Universitario Navale (IUN), Naples. In 1987, he was appointed Associate Professor of Antennas, formerly at the Engineering Faculty of Ancona University and subsequently at the Engineering Faculty of Salerno University. In 1999, he has been appointed Full Professor at the same University. The main topics of his scientific activity are: reflector antennas analysis, antenna measurements, diffraction problems, radar cross section evaluations, scattering from surface impedances, application of sampling techniques to electromagnetics and to NF–FF transformations. Dr. Gennarelli is co-author of about 370 scientific papers, mainly in international journals and conference proceedings. In particular, he is co-author of four books on NF–FF transformation techniques. He is reviewer for several international journals and member of the Editorial board of the *Open Electrical and Electronic Engineering Journal* and of the *International Journal of Antennas and Propagation*.

Rocco Guerriero (M'15) received the Laurea degree in Electronic Engineering and the Ph.D. degree in Information Engineering from the University of Salerno in 2003 and 2007, respectively.

Since 2003, he has been with the Research Group in Applied Electromagnetics of University of Salerno, where he is currently an assistant professor of Electromagnetic Fields. His interests include: application of sampling techniques to the efficient reconstruction of electromagnetic fields and to near-field-far-field transformation techniques; antenna measurements; inversion of ill-posed electromagnetic problems; analysis of microstrip reflectarrays; diffraction problems. Dr. Guerriero is co-author of more than 135 scientific papers, mainly in international journals and conference proceedings. He is reviewer for several international journals and member of the Editorial board of the *International Journal of Antennas and Propagation*.

Scott McBride received his BEE degree in 1986 and his MSEE degree in 1992, both from the Georgia Institute of Technology. His masters' concentrations were in DSP, RF, and communications.

From 1982-1999, Mr. McBride was employed by the Georgia Tech Research Institute, AEL/Cross Systems, and then the Boeing Company. These jobs included a wide variety of software and systems assignments, primarily relating to automated antenna measurements, phased-array control, avionics, array-antenna design, radar environment simulators, and RF data links. He has been with MI Technologies since 1999, rising to their top technical level of Senior Staff Engineer. His time at MI Technologies has again included a wide variety of software and systems engineering tasks in the broad category of measuring and processing RF data as a function of position. Mr. McBride is a Senior Member of the Antenna Measurement Techniques Association. He is also a member of three international working groups that are or recently finished producing specifications for testing radomes or antennas. He has over 20 publications, with most of those in the field of antenna measurements.

Massimo Migliozzi received the Laurea degree in electronic engineering from the University of Salerno, in 1999.

He received the Ph.D. degree in Information Engineering at the same University, where at the present time he is a Research fellow in Electromagnetic Fields. His scientific interests include: application of sampling techniques to the efficient reconstruction of electromagnetic fields and to NF–FF transformation techniques; antenna measurements; electromagnetic compatibility; antenna design; diffraction problems. Dr. Migliozzi is co-author of about 100 scientific papers, mainly in international journals and conference proceedings.